

Physics Opportunities with Supernova Neutrinos

*Ninetta Saviano*¹

¹PRISMA Cluster of Excellence and Mainz Institute for Theoretical Physics, Johannes Gutenberg-Universität Mainz, 55099 Mainz, Germany

DOI: <http://dx.doi.org/10.3204/DESY-PROC-2016-05/16>

Core-collapse supernovae (SN) represent a unique laboratory to probe neutrino properties in the extreme conditions offered by a stellar gravitational collapse. The role of astrophysical messengers played by neutrinos during a stellar collapse is largely associated with the signatures imprinted on the observable SN neutrino burst by flavor conversions occurring deep inside the star. At this regard, the dense SN core represents a crucial environment to investigate neutrino flavor mixing in high-density conditions. Indeed, within a radius of a few hundred kilometers, the neutrino gas is so dense to become a “background to itself”, making the neutrino flavor evolution highly non-linear and leading in some situations to surprising and counterintuitive collective phenomena.

1 Introduction

Core-collapse supernovae (SNe) is one of the most energetic and spectacular phenomena in the Universe. They are powerful explosions which mark the violent death of massive stars ($M \gtrsim 8 M_{\odot}$) as they become unstable during the late phases of their evolution. The explosion is driven by a shock wave that eventually ejects the outer mantle of the collapsing star, liberating a gravitational binding energy $E_B \simeq 3 \times 10^{53}$ erg. Remarkably, 99% of this binding energy is carried away by neutrinos and antineutrinos of all the flavors, making a core-collapse SN one of the most powerful neutrino source. Therefore, neutrinos emitted during such a process are a promising tool to probe neutrino mass and mixing properties and to provide valuable information about SN mechanism itself. The neutrino fluxes and spectra are sensitive to many details of SN physics, notably the progenitor mass, the nuclear equation of state, and the occurrence of convection inside and outside the SN core. Originating deep inside the core and passing through the mantle of the star, the neutrino flavor conversions are affected by dense matter on their road through the stellar envelope. Moreover, in the deepest SN regions the neutrino density is so high that can dominate the flavor evolution, eventually producing a surprising collective behavior in the SN neutrino ensemble. As a consequence of these effects, the SN neutrino fluxes reaching the detectors would be deeply modified with respect to the initial ones, carrying fascinating signatures of oscillation effects occurring in the deepest SN regions. Thus detection of a high-statistics neutrino signal from the next nearby SN represents a new frontier in low-energy neutrino physics and astrophysics. For a more detailed treatment see the recent review [1].

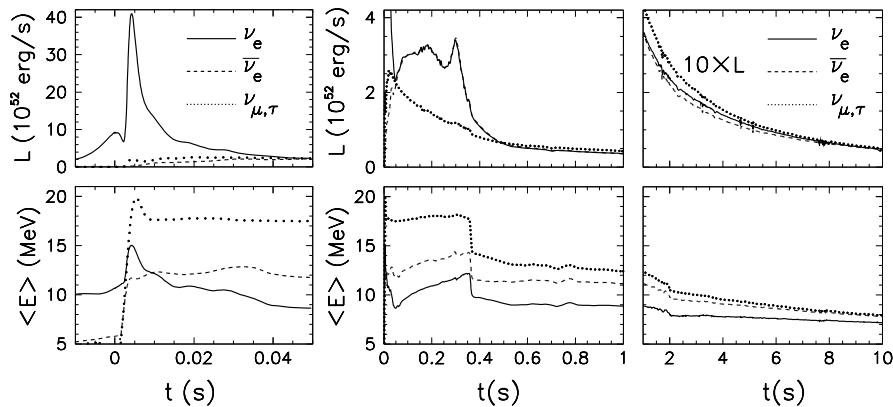


Figure 1: Neutrino signal of a core-collapse SN for a $10.8 M_{\odot}$ progenitor [2]. *Left*: Prompt neutrino burst. *Middle*: Accretion phase. *Right*: Cooling phase.

2 Neutrino emission

During and after the explosion, the star emits neutrinos in three main phases (Fig. 1).

1. *Prompt ν_e burst*: as the shock wave passes through the neutrino sphere, a ν_e burst, lasting $t \simeq 10$ ms, is released due to rapid electron capture on dissociated nuclei (deleptonization of the outer core layers) $e^- + p \rightarrow n + \nu_e$, leading to a sudden rise in the luminosity up to $L = 10^{53}$ erg s^{-1} . The fluxes of the other neutrino flavors are negligible compared to ν_e .
2. *Accretion phase*: the shock wave quickly loses its energy in dissociating nuclei and stagnates at a radius of 150-200 km. Material continues to fall onto the core (*accretion shock*) for the following few 100 ms and powers the emission of neutrinos and antineutrinos of all species, with a luminosity of $L = 10^{52}$ erg s^{-1} and characterized by a strong excess of the ν_e species over the others. Pronounced hierarchy of average energies $\langle E_{\nu_x} \rangle > \langle E_{\bar{\nu}_e} \rangle > \langle E_{\nu_e} \rangle$, where x stands for any of $\nu_{\mu,\tau}$ or $\bar{\nu}_{\mu,\tau}$.
3. *Kelvin-Helmholtz cooling phase*: after the successful explosion, the remaining proto-neutron star cools by neutrino emission over about 10 s. The luminosity is approximately equipartitioned between different species $L = 3 \times 10^{51}$ erg s^{-1} and the flavor hierarchy of average energies is probably mild.

A supernova can be roughly considered as a black-body that cools via neutrino emission. Indeed, supernova simulations typically provide neutrinos emitted with “quasi-thermal” spectra. The spectral characteristics evolve in time, are expected to vary for different supernova progenitors and depend on uncertain input physics such as the nuclear equation of state and the treatment of neutrino transport. Typically, one expects $\langle E_{\nu_e} \rangle \simeq 10$ –12 MeV, $\langle E_{\bar{\nu}_e} \rangle \simeq 12$ –15 MeV, and $\langle E_{\nu_x} \rangle \simeq 15$ –18 MeV.

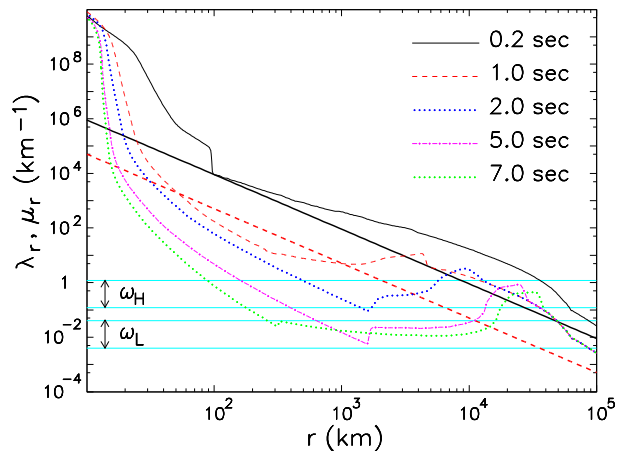


Figure 2: Snapshots of SN potentials for different post-bounce times. Continuous curves refer to the matter potential λ , dot-dashed to the neutrino potential μ (quoted in km^{-1}). Figure from [1].

3 Supernova potential profiles

Effects of flavor conversions on supernova neutrinos depend on the different densities encountered by neutrinos in their propagation in the stellar envelope. In Fig. 2 is represented a snapshot of the different interaction potentials associated with different supernova densities obtained from the Basel-Darmstadt simulations of a $10.8 M_{\odot}$ SN progenitor for different post-bounce times [2]. Self-induced neutrino oscillations, associated with the neutrino-neutrino interactions are related to the neutrino number densities through the neutrino-neutrino potential (Fig. 2)

$$\mu = \sqrt{2}G_F[n_{\nu_e} - n_{\bar{\nu}_e}] = \frac{1}{4\pi r^2} \left(\frac{L_{\nu_e}}{\langle E_{\nu_e} \rangle} - \frac{L_{\bar{\nu}_e}}{\langle E_{\bar{\nu}_e} \rangle} \right), \quad (1)$$

which decreases in time as the SN cools.

Matter effects on SN neutrinos depend on the potential

$$\lambda = \sqrt{2}G_F n_e, \quad (2)$$

where n_e is the net electron density n_e encountered by neutrinos in their propagation. The SN electron density profile is non-monotonic and time-dependent and presents an abrupt discontinuity, corresponding to the position of the shock-front. The two horizontal strips represent the regions associated with MSW resonant flavor conversions with the atmospheric oscillation frequency ω_H (violet band) and with the solar one ω_L (light blue) for an energy range $E \in [1 - 50]$ MeV.

From the comparison of the different densities we realize that in the deepest SN regions ($r < 10^3$ km) $n_{\nu} \gg n_e$, except during the accretion phase ($t < 0.5$ s). When the neutrino density dominates over the matter one (as during the cooling phase) self-induced flavor conversions would develop without any hindrance.

Conversely, at larger radii, the flavor conversions will be dominated by the ordinary matter effects.

4 SN neutrino flavor conversions

4.1 Three-neutrino oscillation framework

The evidence for flavor evolution comes from a series of experiments performed in about four decades of research with very different neutrino beams and detection techniques. Except for few controversial results from short-baseline neutrino experiments, that point towards the existence of extra sterile neutrino states (with $m \sim O(1)$ eV), all the data from the experiments are consistent with the simplest extension of the standard electroweak model needed to accommodate non-zero neutrino masses and mixings. Namely, three flavor eigenstates $\nu_{e,\mu,\tau}$ are mixed with the three mass eigenstates $\nu_{1,2,3}$ through a unitary matrix U , which in terms of one-particle neutrino states $|\nu\rangle$, is defined as $|\nu_\alpha\rangle = \sum_{i=1}^3 U_{\alpha i}^* |\nu_i\rangle$.

A common parametrization for the matrix U is [3]:

$$U = \begin{pmatrix} 1 & 0 & 0 \\ 0 & c_{23} & s_{23} \\ 0 & -s_{23} & c_{23} \end{pmatrix} \begin{pmatrix} c_{13} & 0 & s_{13}e^{-i\delta} \\ 0 & 1 & 0 \\ -s_{13}e^{i\delta} & 0 & c_{13} \end{pmatrix} \begin{pmatrix} c_{12} & s_{12} & 0 \\ -s_{12} & c_{12} & 0 \\ 0 & 0 & 1 \end{pmatrix} \quad (3)$$

with $c_{ij} = \cos\theta_{ij}$ and $s_{ij} = \sin\theta_{ij}$, θ_{ij} being the mixing angles and $\delta \in [0, 2\pi]$ being the CP-violating phase¹.

The three-neutrino mass spectrum $\{m_i\}_{i=1,2,3}$ is characterized by a “doublet” of relatively close states and by a third “lone” neutrino state, which may be either heavier than the doublet (“normal hierarchy,” NH) or lighter (“inverted hierarchy,” IH). Typically, the lightest (heaviest) neutrino in the doublet is called ν_1 (ν_2) and the corresponding mass squared difference is defined as

$$\delta m^2 = m_2^2 - m_1^2 > 0 \quad (4)$$

by convention. The δm^2 is traditionally named the *solar* mass squared difference. The lone state is then labeled as ν_3 , and the physical sign of $m_3^2 - m_{1,2}^2$ distinguishes NH from IH. The second independent squared mass difference Δm^2 , called also *atmospheric* mass squared difference, is

$$\Delta m^2 = \left| m_3^2 - \frac{m_1^2 + m_2^2}{2} \right|, \quad (5)$$

so that the two hierarchies (NH and IH) are simply related by the transformation $+\Delta m^2 \rightarrow -\Delta m^2$. Numerically, it results that $\delta m^2 \ll \Delta m^2$.

The latest solar, reactor and long-baseline neutrino oscillation analyses indicate the following $\pm 2\sigma$ ranges for each parameter (95% C.L.) taken from [4]

$$\begin{aligned} \Delta m^2 &= (2.43_{-0.13}^{+0.12}) \times 10^{-3} \text{ eV}^2, & \delta m^2 &= (7.54_{-0.39}^{+0.46}) \times 10^{-5} \text{ eV}^2, \\ \sin^2 \theta_{12} &= (3.08_{-0.34}^{+0.17}) \times 10^{-1}, & \sin^2 \theta_{23} &= (4.37_{-0.44}^{+1.15}) \times 10^{-1}, & \sin^2 \theta_{13} &= (2.34_{-0.39}^{+0.40}) \times 10^{-2}. \end{aligned} \quad (6)$$

Within the three-neutrino scenario, the most important unsolved problems require probing the CP-violating phase δ , the mass hierarchy, and the absolute neutrino masses. In this context, a high-statistics detection of Galactic SN neutrinos could give a unique help to solve some of these open issues.

¹We neglect here extra-phases possible if neutrinos are Majorana particles, since they are not relevant in oscillations.

4.2 Self-induced flavor evolution of SN neutrinos

Neutrinos free streaming beyond the neutrinosphere also interact among themselves (*neutrino self-interactions*). As pointed out in seminal papers [5, 6], in the deepest regions of a SN the neutrino gas is so dense that neutrinos themselves form a background medium triggering large *self-induced* flavor conversions in the deepest SN regions [7]. Under these circumstances, neutrinos emitted with different energies would be locked to oscillate in a collective fashion.

The neutrino-neutrino interactions make an additional contribution to the refractive energy shift in the neutrino propagation. This term is proportional to the neutrino density making the equations of motion non linear and so numerically challenging. The main complication in the ν - ν refractive term for SN neutrinos is the angular term coming from the current-current nature of the weak interactions. Consequently, for the non-isotropic neutrino emission from the SN core this velocity-dependent term would produce a net current that leads to a different refractive index for neutrinos that propagate on different trajectories. This is at the origin of the so-called “multi-angle effects” [7].

The multi-angle flavor evolution described by non-linear partial differential equations, has not been solved in its full complexity until now.

A few years ago multi-angle simulations were developed within the so-called “*bulb model*” where it is assumed that neutrinos are emitted uniformly and half-isotropically (i.e., with all the outward-going modes occupied, and all the backward going modes empty) from the surface of a spherical neutrinosphere, like in a blackbody. Moreover, it is assumed that there is azimuthal symmetry of the neutrino emission at the neutrinosphere and that all the physical conditions in the star only depend on the distance from the center of the star. Despite the numerous studies on the subject, at the moment a complete picture of the self-induced flavor conversions in SNe is still missing. Indeed, it has been recently questioned if removing some of the symmetries assumed in this model, this would trigger new instabilities in the flavor evolution. By means of a stability analysis of the linearized neutrino EoMs [8], it has been pointed out that removing the assumption of axial symmetry in the ν propagation, a new multi-azimuthal-angle (MAA) instability could emerge in the flavor evolution of the dense SN neutrino gas. The presence of MAA effects unavoidably implies the breaking of the spherical symmetry in the flavor evolution after the onset of the flavor conversions. This would lead to a challenging multi-dimensional problem involving partial differential equations. The MAA instability has shown as self-interacting neutrinos can *spontaneously break* the symmetries of the initial conditions. Such insight stimulated further investigations about the validity of the solution of the SN neutrino EoMs worked out within the bulb model. It has been recently realized that instabilities may grow once initial symmetries are relaxed, since self-interacting neutrinos can spontaneously break the translation symmetries in time [9, 10, 11] and space.

4.3 Suppression of collective oscillations

Predictions are more robust in the phases where collective effects are suppressed, i.e.:

- *Neutronization burst* ($t < 20$ ms), where the ν_e flux is strongly enhanced with respect to ν_x , while the $\bar{\nu}_e$ flux is strongly suppressed.
- *Accretion phase*, where $n_{e^-} - n_{e^+} \gg n_{\bar{\nu}_e} - n_{\bar{\nu}_x}$. The multi-angle matter effects could produce a large spread in the oscillation frequencies for neutrinos travelling on different trajectories, blocking the self-induced flavor conversions. Dedicated studies have been

performed in [12, 13, 14, 15, 16, 17] using inputs from recent hydrodynamic SN simulations. It has been found that the large matter term inhibits the development of collective oscillations at early times for iron-core SNe. The matter suppression of self-induced effects for iron-core SNe makes relatively easy the prediction of the oscillation effects during the accretion phase, since the neutrino fluxes will be processed by the only MSW matter effects. As a consequence, the detection of the SN neutrino signal at early times is particularly relevant for the mass hierarchy discrimination.

5 Observable signatures of SN neutrino flavor conversions

We present some of the possible observable signatures of flavor conversions in SNe and their sensitivity to the neutrino mass hierarchy. For definitiveness, we will refer to a Galactic SN at a distance $d = 10$ kpc from the Earth.

(a) Self-induced spectral splits. Observationally, the most important consequence of the self-induced flavor conversions is a swap of the ν_e and $\bar{\nu}_e$ spectrum with the non-electron species ν_x and $\bar{\nu}_x$ in certain energy intervals, and the resultant spectral splits at the edges of these swap intervals. Some of the spectral splits could occur sufficiently close to the peak energies to produce significant distortions in the SN neutrino signal, observable in the large underground detectors.

(b) Neutrinos from the SN neutronization burst. The ν_e neutronization burst is a particularly interesting probe of flavor conversions, since it can be considered almost as a “standard candle” being independent of the mass progenitor and nuclear EoS. Since self-induced effects are not operative on the SN ν_e neutronization burst, the ν_e flux would be only affected by MSW effects. At the very early post-bounce times relevant for the prompt burst, MSW flavor conversions would occur along the static progenitor matter density profile. We expect that the observable ν_e flux at Earth would be

$$F_{\nu_e} = F_{\nu_x}^0 \quad (\text{NH}) , \quad (7)$$

$$F_{\nu_e} = \sin^2 \theta_{12} F_{\nu_e}^0 + \cos^2 \theta_{12} F_{\nu_x}^0 \quad (\text{IH}) . \quad (8)$$

The observation of the neutronization peak would indicate the inverted mass hierarchy, while we do not expect its detection in NH. Concerning the possibility to detect the ν_e neutronization burst, while Mton class WC detectors measure predominantly the $\bar{\nu}_e$ flux using inverse beta decay, they are also sensitive to the subdominant ν_e channel via elastic scatterings on e^- (see Fig.). On the other hand, a large LAr TPC will make the cleanest identification of the prompt ν_e burst through its unique feature of measuring ν_e charged-current interactions, enabling to probe oscillation physics during the early stage of the SN explosion.

(c) Earth matter effect to discriminate the mass hierarchy. For the SN neutrinos reaching the detector from “below”, the Earth crossing would induce an energy-dependent modulation in the neutrino survival probability. The appearance of the Earth effect depends on the neutrino fluxes and on the mixing scenario. In particular, the Earth matter effect should be present for antineutrinos in NH and for neutrinos in IH, providing a potential tool to distinguish between these two cases. The accretion phase is particularly promising to detect Earth crossing signatures because the absolute SN ν flux is large and the flavor-dependent flux differences are also large.

(d) Rise time of the neutrino signal. The rise time of a Galactic iron-core SN $\bar{\nu}_e$ light curve, observable in large underground detectors, can provide a diagnostic tool for the

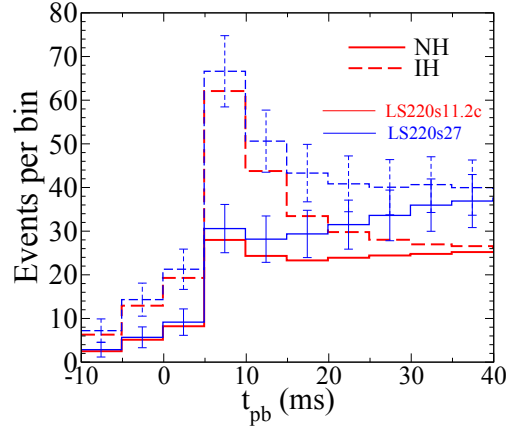


Figure 3: Neutronization events rate per time bin in a 560-kton WC detector for $27 M_{\odot}$ and $11 M_{\odot}$ SN progenitors at $d = 10$ kpc for both NH (continuous curve) and IH (dashed curve).

neutrino mass hierarchy. Due to the combination of matter suppression of collective effects at early post-bounce times and the presence of the ordinary MSW effect in the outer layers of the SN, one expects that the observable $\bar{\nu}_e$ flux at Earth would be given by

$$F_{\bar{\nu}_e} = \cos^2 \theta_{12} F_{\bar{\nu}_e}^0 + \sin^2 \theta_{12} F_{\bar{\nu}_x}^0 \quad (\text{NH}) , \quad (9)$$

$$F_{\bar{\nu}_e} = F_{\bar{\nu}_x}^0 \quad (\text{IH}) . \quad (10)$$

It is clear that the $F_{\bar{\nu}_e}$ flux at the Earth would basically reflect the original $F_{\bar{\nu}_x}^0$ flux if IH occurs, or closely match the $F_{\bar{\nu}_e}^0$ flux in NH. Figure 4 shows the expected *overall* signal rate $R(t)$ in the IceCube detector for a Galactic SN.

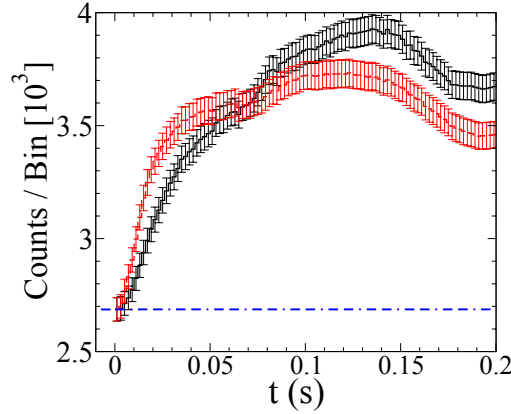


Figure 4: Supernova signal in IceCube assuming a distance of 10 kpc, based on a simulation for a $15 M_{\odot}$ SN progenitor from the Garching group. Figure from [1].

6 Acknowledgments

N.S. have received funding from the European Research Council (ERC) under the European Union's Horizon 2020 research and innovation programme (grant agreement No. 637506, “ ν Directions”).

References

- [1] A. Mirizzi, I. Tamborra, H. T. Janka, N. Saviano, K. Scholberg, R. Bollig, L. Hudepohl and S. Chakraborty, Riv. Nuovo Cim. **39** (2016) no.1-2, 1.
- [2] T. Fischer, S. C. Whitehouse, A. Mezzacappa, F.-K. Thielemann and M. Liebendorfer, Astron. Astrophys. **517** (2010) A80.
- [3] G. L. Fogli, E. Lisi, A. Marrone and A. Palazzo, Prog. Part. Nucl. Phys. **57**, 742 (2006).
- [4] F. Capozzi, G. L. Fogli, E. Lisi, A. Marrone, D. Montanino and A. Palazzo, Phys. Rev. D **89**, 093018 (2014).
- [5] J. T. Pantaleone, Phys. Rev. D **46** (1992) 510.
- [6] J. T. Pantaleone, Phys. Lett. B **342** (1995) 250.
- [7] H. Duan, G. M. Fuller, J. Carlson and Y. Z. Qian, Phys. Rev. Lett. **97**, 241101 (2006).
- [8] G. G. Raffelt, S. Sarikas and D. de Sousa Seixas, Phys. Rev. Lett. **111**, no. 9, 091101 (2013) [Erratum-ibid. **113**, no. 23, 239903 (2014)].
- [9] G. Mangano, A. Mirizzi and N. Saviano, Phys. Rev. D **89**, no. 7, 073017 (2014).
- [10] S. Abbar and H. Duan, Phys. Lett. B **751**, 43 (2015).
- [11] B. Dasgupta and A. Mirizzi, Phys. Rev. D **92**, no. 12, 125030 (2015).
- [12] S. Chakraborty, T. Fischer, A. Mirizzi, N. Saviano and R. Tomàs, Phys. Rev. Lett. **107**, 151101 (2011) [arXiv:1104.4031 [hep-ph]].
- [13] S. Chakraborty, T. Fischer, A. Mirizzi, N. Saviano and R. Tomàs, Phys. Rev. D **84**, 025002 (2011).
- [14] B. Dasgupta, E. P. O'Connor and C. D. Ott, Phys. Rev. D **85**, 065008 (2012).
- [15] S. Sarikas, G. G. Raffelt, L. Hudepohl and H. T. Janka, Phys. Rev. Lett. **108**, 061101 (2012)
- [16] N. Saviano, S. Chakraborty, T. Fischer and A. Mirizzi, Phys. Rev. D **85**, 113002 (2012).
- [17] S. Chakraborty, A. Mirizzi, N. Saviano and D. d. S. Seixas, Phys. Rev. D **89**, no. 9, 093001 (2014).